Inorg. Chem. **2005**, *44*, 8707−8714

C- and Z-Shaped Coordination Compounds. Synthesis, Structure, and Spectroelectrochemistry of *cis*- and *trans*-$[Re(CO)_3(L)]_2$-2,2′-bisbenzimidizolate with L = 4-Phenylpyridine, 2,4′-Bipyridine, or Pyridine

Peter H. Dinolfo, Kurt D. Benkstein, Charlotte L. Stern, and Joseph T. Hupp*

Department of Chemistry, Northwestern University, 2145 Sheridan Road, Evanston, Illinois 60208-3113

Received June 2, 2005

A series of C- and Z-shaped complexes of the form *cis*- and *trans*-$[Re(CO)_3(L)]_2$BiBzIm, where L = 4-phenylpyridine, 2,4′-bipyridine, or pyridine and BiBzIm = 2,2′-bisbenzimidizolate, have been synthesized by the reaction of $[Re(CO)_4]_2$BiBzIm with a slight excess of L in refluxing tetrahydrofuran. Five of the six compounds have been isolated and crystallographically and electrochemically characterized. Formation of the sixth, the cis form of the $[Re(CO)_3$(4-phenylpyridine)$]_2$BiBzIm, is evidently inhibited by the torsional steric demands of proximal 4-phenylpyridines. The compounds are acyclic analogues of recently studied tetrarhenium molecular rectangles and are of interest, in part, because of their potential to form ligand-centered mixed-valence (LCMV) compounds upon reduction by one electron. Spectroelectrochemical measurements corroborated the formation of a LCMV version of *cis*-$[Re(CO)_3(L)]_2$BiBzIm but failed to uncover a ligand-based intervalence transition. Electrochemical measurements revealed isomer-dependent L/L electrostatic effects, resulting in greater mixed-valence ion comproportionation for C-shaped assemblies versus Z-shaped assemblies.

Introduction

We have recently reported on the use of rhenium-based molecular rectangles[1−10] as organizational motifs for the investigation of intramolecular electron transfer. Examined were tetrarhenium assemblies that configure pairs of redox-active ligands, LL, in reasonably well-defined, largely cofacial geometries. As shown in Scheme 1, when one LL ligand is reduced, the rectangles comprise ligand-centered mixed-valence (LCMV) compounds.[1−3] We find that electronic coupling in these systems is dominated by direct donor-orbital/acceptor-orbital overlap, rather than metal-mediated superexchange. In other words, the role of the metals is limited mainly to a structural one with the assemblies behaving electronically as two-state systems. Depending on the identity of LL and the precise positioning of LL pairs with respect to each other, we find that electronic coupling can range from undetectably weak to sufficiently strong so that full valence delocalization occurs. In most cases but not all, one or more intervalence transfer (IT) bands can be detected in the electronic absorption spectrum. As with other mixed-valence compounds, if the LCMV assembly's odd electron is localized, the IT band intensity and energy can report directly on the electronic coupling energy and the reorganization energy for the corresponding thermal intramolecular electron exchange reaction.[11,12]

* To whom correspondence should be addressed. E-mail: jthupp@chem.northwestern.edu.

(1) Dinolfo, P. H.; Williams, M. E.; Stern, C. L.; Hupp, J. T. *J. Am. Chem. Soc.* **2004**, *126*, 12989−13001.
(2) Dinolfo, P. H.; Hupp, J. T. *J. Am. Chem. Soc.* **2004**, *126*, 16814−16819.
(3) Dinolfo, P. H.; Lee, S. J.; Coropceanu, V.; Brédas, J.-L.; Hupp, J. T. *Inorg. Chem.* **2005**, *44*, 5789−5797.
(4) Hartmann, H.; Berger, S.; Winter, R.; Fiedler, J.; Kaim, W. *Inorg. Chem.* **2000**, *39*, 4977−4980.
(5) Woessner, S. M.; Helms, J. B.; Shen, Y.; Sullivan, B. P. *Inorg. Chem.* **1998**, *37*, 5406−5407.
(6) Benkstein, K. D.; Hupp, J. T.; Stern, C. L. *Inorg. Chem.* **1998**, *37*, 5404−5405.
(7) Benkstein, K. D.; Hupp, J. T.; Stern, C. L. *J. Am. Chem. Soc.* **1998**, *120*, 12982−12983.
(8) Thanasekaran, P.; Liao, R. T.; Liu, Y. H.; Rajendran, T.; Rajagopal, S.; Lu, K. L. *Coord. Chem. Rev.* **2005**, *249*, 1085−1110.
(9) Benkstein, K. D.; Stern, C. L.; Splan, K. E.; Johnson, R. C.; Walters, K. A.; Vanhelmont, F. W. M.; Hupp, J. T. *Eur. J. Inorg. Chem.* **2002**, *2002*, 2818−2822.
(10) Benkstein, K. D.; Hupp, J. T.; Stern, C. L. *Angew. Chem., Int. Ed.* **2000**, *39*, 2891−2893.
(11) Hush, N. S. *Prog. Inorg. Chem.* **1967**, *8*, 391−444.
(12) Hush, N. S. *Coord. Chem. Rev.* **1985**, *64*, 135−157.

10.1021/ic050894u CCC: $30.25
Published on Web 10/27/2005

Scheme 1

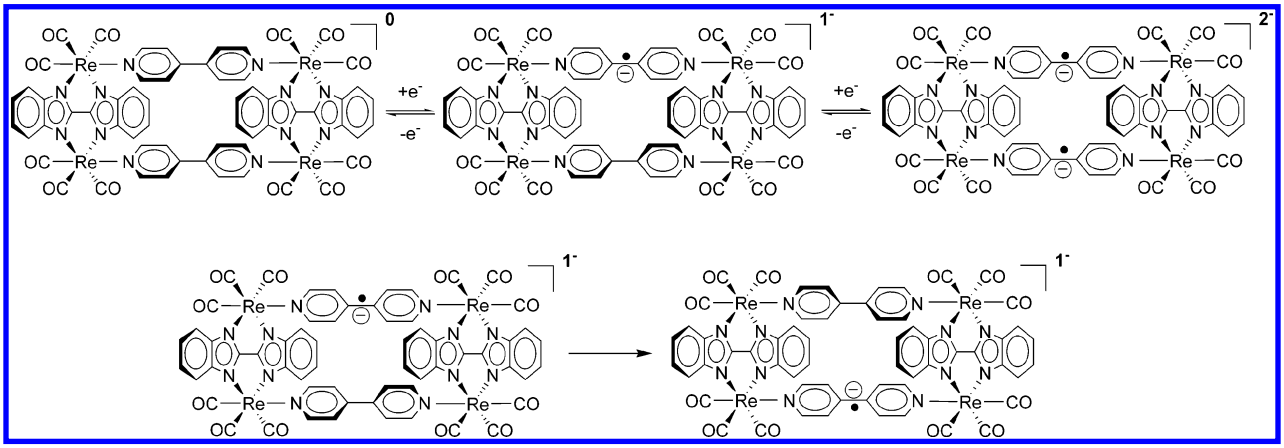

Chart 1

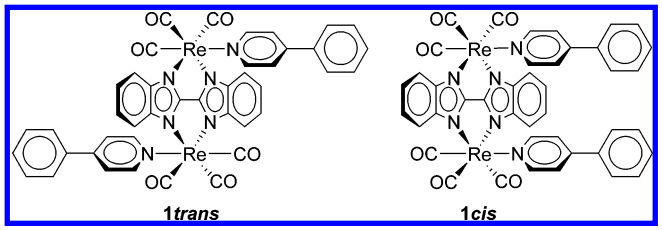

With these observations in mind, we reasoned that analogous acyclic C- and Z-shaped compounds might also display LCMV behavior. Examples are the dirhenium 2,2′-bisbenzimidazolate (BiBzIm) compounds, **1cis** and **1trans**, shown in Chart 1. We further reasoned that, given the comparative *un*importance of superexchange coupling in the LCMV rectangles, large differences in intramolecular electronic coupling might be encountered for C-shaped versus Z-shaped assemblies. Although not investigated here, we also reasoned that open-ended C-shaped assemblies, in contrast to BiBzIm-based rectangles, might be sufficiently pliable to accommodate planar guest molecules, such as LL/LL intercalants, potentially permitting noncovalent "through matter" electronic coupling behavior to be investigated.[13−18]

Outlined here are the synthesis, X-ray structural characterization, electrochemical behavior, and electronic spectral properties of an almost complete series of *cis*- and *trans*-$[Re(CO)_3(L)]_2$BiBzIm compounds, where L = 4-phenylpyridine (4-PhPy), 2,4′-bipyridine (2,4′-bpy), or pyridine. In two of the three cases, the syntheses yielded isolatable quantities of both isomers, with separation obtained by thin-layer chromatography (TLC). In some cases, transiently reversible stepwise reduction of L/L pairs within a given assembly was observed, implying the formation of LCMV species. The measurements provide evidence for the expected isomer-dependent electrostatic interactions. Unfortunately, however, the reduced assemblies proved insufficiently stable for L/L IT bands to be detected in the visible or near-infrared (NIR) spectrum.

Experimental Section

General Methods. Infrared spectra were recorded on a Bio-Rad FTS-40 Fourier transform infrared spectrometer. All NMR spectra were recorded on either a Varian Mercury 400-MHz spectrometer or a Varian INOVA 500-MHz spectrometer, and the chemical shifts were referenced to the standard solvent shift. Low resolution mass spectrometry−fast atom bombardment (LRMS−FAB) and high resolution mass spectrometry−FAB (HRMS−FAB) were obtained in the Mass Spectrometry Laboratory of the School of Chemical Sciences, University of Illinois. UV−visible absorption spectra were recorded with a Varian Cary 5000 spectrophotometer.

Materials. All commercial reagents were of ACS grade and used without further purification. Tetrahydrofuran (THF) and methylene chloride were purified using a two-column solid-state purification system (Glasscontour System, Joerg Meyer, Irvine, CA). 4-PhPy and 2,4′-bpy were purchased from Aldrich, and pyridine was obtained from Fisher Scientific. Whatman preparatory TLC plates (150-Å silica, 1000-μm layer thickness) were used for the separation of cis and trans isomers. **4** was synthesized by previous literature preparations.[10]

***trans*-$[Re(CO)_3(4\text{-PhPy})]_2$BiBzIm (1trans). 4** (65 mg, 0.078 mmol) and 4-PhPy (28 mg, 0.180 mmol) were combined with 80 mL of THF under N_2. The mixture was heated to reflux under N_2 for 24 h. The removal of ∼80% of the solvent and the addition of hexanes gave 74 mg of **1trans**, a light yellow powder after filtration (87% yield). IR confirmed the trans form as the only isomer isolated. ^{1}H NMR (400 MHz, acetone-d_6): 8.42 (d, 4H), 7.88 (q, 4H), 7.66 (q, 4H), 7.62 (d, 4H), and 7.50 (m, 10H). IR (THF, cm^{-1}): 2020 (C≡O), 1915 (C≡O), and 1904 (C≡O). LRMS−FAB (*m*/*z*): $[M]^+$ calcd for $Re_2C_{42}H_{26}O_6N_6$, 1082.1; found, 1082.4. HRMS−FAB (*m*/*z*): $[M]^+$ calcd for $Re_2C_{42}H_{26}O_6N_6$, 1084.1029; found, 1084.1026.

***cis*- and *trans*-$[Re(CO)_3(2,4'\text{-bpy})]_2$BiBzIm (2cis and 2trans). 4** (75 mg, 0.09 mmol) and 2,4′-bpy (30 mg, 0.19 mmol) were combined with 80 mL of THF under N_2. The mixture was heated to reflux under N_2 for 24 h. The removal of ∼80% of the solvent and the addition of hexanes gave 93 mg of **2cis** and **2trans**, a light yellow powder after filtration (94% yield, combined). Preparatory TLC separation using a 100:1 CH_2Cl_2/MeOH mixture gave **2trans** and **2cis** as yellow crystalline powders after recrystallization. **2trans**. Yield = 21 mg. ^{1}H NMR (400 MHz, CD_2Cl_2): 8.63 (d, 2H), 8.36

(13) Troisi, A.; Ratner, M. A.; Zimmt, M. B. *J. Am. Chem. Soc.* **2004**, *126*, 2215−2224.
(14) Zimmt, M. B.; Waldeck, D. H. *J. Phys. Chem. A* **2003**, *107*, 3580−3597.
(15) Kaplan, R.; Napper, A. M.; Waldeck, D. H.; Zimmt, M. B. *J. Phys. Chem. A* **2002**, *106*, 1917−1925.
(16) Kaplan, R. W.; Napper, A. M.; Waldeck, D. H.; Zimmt, M. B. *J. Am. Chem. Soc.* **2000**, *122*, 12039−12040.
(17) Napper, A. M.; Read, I.; Kaplan, R.; Zimmt, M. B.; Waldeck, D. H. *J. Phys. Chem. A* **2002**, *106*, 5288−5296.
(18) Kumar, K.; Lin, Z.; Waldeck, D. H.; Zimmt, M. B. *J. Am. Chem. Soc.* **1996**, *118*, 243−244.

Table 1. Crystallographic Data for **1trans**, **2trans**, **2cis**, **3trans**, **3cis**, and **4**

compound	**1trans** + 1.5 × THF + hexane	**2trans** and **2cis**	**3trans**	**3cis**	**4**
empirical formula	$Re_3C_{75}H_{65}N_9O_{10.5}$	$Re_3C_{60}H_{36}N_{12}O_9$	$Re_2C_{30}H_{18}N_6O_6$	$Re_2C_{30}H_{18}N_6O_6$	$Re_2C_{22}H_8N_4O_8$
formula weight	1818.96	1627.61	930.92	930.92	828.74
crystal color, habit	yellow, plate	colorless, prismatic	yellow, plate	colorless, polyhedron	colorless, columnar
crystal dimensions (mm)	0.93 × 0.54 × 0.50	0.08 × 0.09 × 0.22	0.30 × 0.28 × 0.10	0.05 × 0.08 × 0.08	0.52 × 0.23 × 0.18
crystal system	monoclinic	monoclinic	monoclinic	tetragonal	tetragonal
space group	$P2_1/n$ (No. 14)	$P2_1/n$ (No. 14)	$P2_1/n$ (No. 14)	$I\bar{4}2d$ (No. 122)	$I4_1/a$ (No. 88)
a (Å)	12.244(I)	10.986(2)	9.079(2)	14.697(18)	21.362(2)
b (Å)	27.632(1)	19.522(3)	16.653(3)		
c (Å)	22.478(1)	25.768(4)	9.459(2)	26.136(5)	9.784(2)
β (deg)	95.050(1)	97.593(2)	91.161(3)		
V (Å^3)	7575.64(4)	5477.8(15)	1429.8(5)	5645.3(12)	4464.5(13)
Z	4	4	2	8	8
T (K)	153	153	153	153	153
ρ (calcd, g/cm^3)	1.538	1.974	2.162	2.191	1.23
μ (mm^{-1})	4.843	6.684	8.514	8.626	10.894
goodness of fit on F^2	0.961	1.064	1.041	1.063	1.198
R (F)[a]	0.042	0.033	0.022	0.029	0.021
R_w (F^2)[b]	0.096	0.071	0.052	0.057	0.046

[a] $R(F) = \sum||F_o| - |F_c||/\sum|F_o|$. [b] $R_w(F^2) = [\sum w(F_o^2 - F_c^2)^2]/[\sum w(F_o^2)^2]^{1/2}$.

(d, 4H), 7.87 (q, 4H), 7.75 (t, 2H), 7.72 (d, 4H), 7.65 (d, 2H), 7.43 (q, 4H), and 7.32 (d, 2H). IR (THF, cm^{-1}): 2020 (C≡O), 1916 (C≡O), and 1904 (C≡O). LRMS−FAB (*m*/*z*): [M]$^+$ calcd for $Re_2C_{40}H_{24}O_6N_8$, 1086.1; found, 1086.4. HRMS−FAB (*m*/*z*): [M]$^+$ calcd for $Re_2C_{40}H_{24}O_6N_8$, 1086.0934; found, 1086.0933. **2cis**. Yield = 19 mg. ^{1}H NMR (400 MHz, CD_2Cl_2): 8.30 (d, 2H), 8.07 (d, 4H), 7.89 (q, 4H), 7.45 (q, 4H), 7.39 (t, 2H), 7.33 (d, 4H), 7.16 (d, 2H), and 7.07 (t, 2H). IR (THF, cm^{-1}): 2027 (C≡O), 2019 (C≡O), 1918 (C≡O), and 1903 (C≡O). LRMS−FAB (*m*/*z*): [M]$^+$ calcd for $Re_2C_{40}H_{24}O_6N_8$, 1086.1; found, 1086.5. HRMS−FAB (*m*/*z*): [M]$^+$ calcd for $Re_2C_{40}H_{24}O_6N_8$, 1086.0934; found, 1086.0933.

***cis*- and *trans*-[Re(CO)$_3$(pyridine)]$_2$BiBzIm (3cis and 3trans).** **4** (150 mg, 0.181 mmol) and pyridine (0.030 mL, 30 mg, 0.380 mmol) were combined with 175 mL of THF under N_2. The mixture was heated to reflux under N_2 for 24 h. The removal of ∼80% of the solvent and the addition of hexanes gave 154 mg of **3cis** and **3trans**, a light yellow powder after filtration (91% yield, combined). Preparatory TLC separation using a 50:50 THF/hexanes mixture gave **3trans** and **3cis** as yellow crystalline powders after recrystallization. **3trans**. Yield = 66 mg. ^{1}H NMR (400 MHz, $CDCl_3$): 8.00 (d, 4H), 7.83 (q, 4H), 7.41 (q, 4H), 7.34 (t, 2H), and 6.72 (t, 4H). IR (CH_2Cl_2, cm^{-1}): 2021 (C≡O), 1914 (C≡O), and 1902 (C≡O). LRMS−FAB (*m*/*z*): [M]$^+$ calcd for $Re_2C_{30}H_{18}O_6N_6$, 930.9; found, 931.1. HRMS−FAB (*m*/*z*): [M]$^+$ calcd for $Re_2C_{30}H_{18}O_6N_6$, 932.0403; found, 932.0404. **3cis**. Yield = 45 mg. ^{1}H NMR (400 MHz, $CDCl_3$): 8.26 (d, 4H), 7.82 (q, 4H), 7.59 (t, 2H), 7.39 (q, 4H), and 7.06 (t, 4H). IR (CH_2Cl_2, cm^{-1}): 2028 (C≡O), 2021 (C≡O), 1917 (C≡O), and 1901 (C≡O). LRMS−FAB (*m*/*z*): [M]$^+$ calcd for $Re_2C_{30}H_{18}O_6N_6$, 930.9; found, 931.0. HRMS−FAB (*m*/*z*): [M]$^+$ calcd for $Re_2C_{30}H_{18}O_6N_6$, 932.0403; found, 932.0404.

Crystal Structure Determinations. Crystals of **1trans**, **2trans**, **2cis**, **3trans**, and **3cis** were grown from the slow diffusion of hexane into saturated THF solutions. For **2trans** and **2cis**, the unseparated reaction product was used, resulting in isomer cocrystallization. Crystals of **4** were obtained from the slow evaporation of a saturated CH_2Cl_2 solution. The crystals were mounted on glass fibers using oil and immediately placed in a cold nitrogen stream at 153 K. Data collection was done using a Bruker Smart 1000 charge-coupled device diffractometer with Mo Kα radiation (λ = 0.710 69 Å). Data were processed using the SMART and SAINT programs.[19] An analytical integration absorption correction was applied to all data, and the data for **3trans** were corrected for secondary extinction.

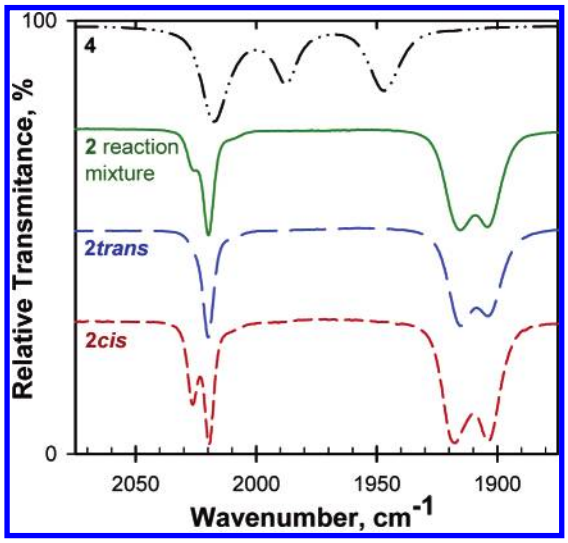

Figure 1. Carbonyl stretching region of the IR spectra for **4** (dashed−dotted black line), a reaction mixture of **2** (solid green line), **2trans** (long dashed blue line), and **2cis** (short dashed red line) in THF.

The structures were solved by direct methods, and refinement was done using the SHELXT crystallographic software package.[20] The refinements of all structures were relatively straightforward. For all structures, non-hydrogen atoms were refined anisotropically and hydrogen atoms were added in idealized positions. The structure for compound **1trans** contained two disordered THF molecules and one disordered hexane molecule of which only one of the THF solvent molecules was refined anisotropically; the remaining solvent molecules were refined isotropically. Crystal descriptions and sizes along with structure refinement data are shown in Table 1. X-ray crystallographic files (CIF) are included in Supporting Information. Oak Ridge thermal-ellipsoid plot (ORTEP) drawings of **1trans**, **2trans**, **2cis**, **3trans**, **3cis**, and **4** are shown in Figure 1. Table 2 contains Re−N bond distances.

(19) *SMART*, version 5.054; data collection; Bruker Analytical X-ray Instruments, Inc.: Madison, WI, 2000. *SAINT-Plus*, version 6.02A; data processing software for the SMART System; Bruker Analytical X-ray Instruments, Inc.: Madison, WI, 2000.
(20) Sheldrick, G. M. *SHELXTL*, DOS/Windows/NT version 5.10; Bruker Analytical X-ray Instruments, Inc.: Madison, WI, 1997.

Scheme 2

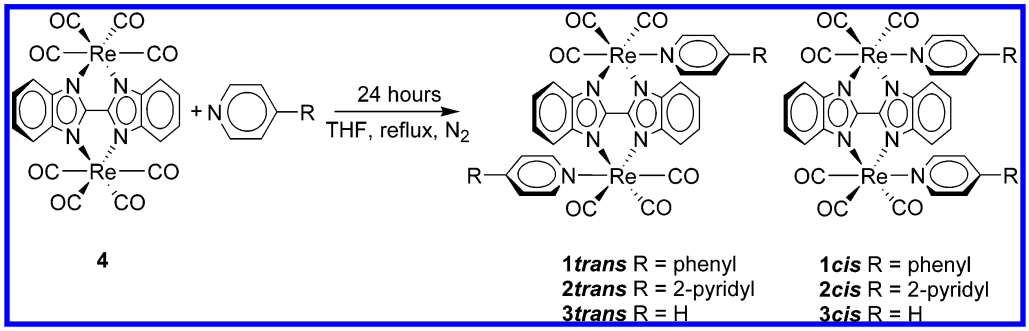

Electrochemical Measurements. All cyclic voltammetric and differential pulse voltammetric experiments were performed and analyzed using a CHI900 (CH Instruments, Austin, TX) potentiostat. Electrolyte solutions [0.1 M tetrabutylammonium hexafluorophosphate ($TBAPF_6$; >99%, Fluka)] were prepared with anhydrous THF and were nitrogen degassed prior to use. A Pt wire was used as the counter electrode, and 2-mm-diameter Pt or Au macro disk electrodes were used as the working electrodes. A silver wire was used as a pseudo-reference electrode with ferrocene (Aldrich, purified by sublimation) added as an internal reference at the end of each experiment. All experiments were run under a nitrogen atmosphere. UV/visible/NIR spectroelectrochemical (SEC) experiments were carried out as previously described.[1]

Table 2. Re−N Bond Distances for **1trans**, **2trans**, **2cis**, **3trans**, **3cis**, and **4**

	bond lengths (Å)			
	LL pyridyl N−Re		imidazolyl N−Re	
1trans	Re1−N9	2.212(2)	Re1−N4	2.223(2)
			Re1−N5	2.220(2)
	Re2−N1	2.195(2)	Re2−N2	2.206(2)
			Re2−N3	2.212(2)
	Re3−N8	2.180(2)	Re3−N6	2.216(2)
			Re3−N7	2.206(2)
2trans	Re3−N9	2.220(4)	Re3−N7	2.239(4)
			Re3−N8	2.2179(4)
2cis	Re1−N5	2.2099(4)	Re1−N1	2.2139(3)
			Re1−N3	2.2299(3)
	Re2−N6	2.203(3)	Re2−N2	2.203(3)
			Re2−N4	2.214(3)
3trans	Re1−N3	2.223(2)	Re1−N1	2.210(2)
			Re1−N2	2.226(2)
3cis	Re1−N3	2.205(5)	Re1−N1	2.196(5)
			Re1−N2	2.220(5)
4			Re1−N1	2.208(3)
			Re1−N2	2.209(3)
average		2.21(1)		2.22(1)

Results and Discussion

Synthesis and Characterization. The general preparative procedure for **1**−**3** is shown in Scheme 2. A slight excess of a pyridine-based ligand is combined with **4** in refluxing THF under N_2 for approximately 24 h. The reactions are monitored by IR for the disappearance of the carbonyl stretches of **4** at 2111, 2017, 1988, and 1946 cm^{-1} and the appearance of carbonyl stretches for the products. Note that the as-prepared assemblies are neutral, with the dianionic BiBzIm ligand formally charge balancing the pair of Re(I) centers. The reactivity of **4** is a good example of the classic trans labilization of group VII complexes by carbonyl ligands—the effect, arising from competitive π back bonding by a carbonyl, results in the weakening of the opposing M—CO bond.[21−24]

In THF as the solvent, both forms of **2** and **3** were obtained with the ratio of cis to trans varying between 1:1 and 2:3, depending on the concentrations used.[25] Under the mild reaction conditions used here, only the trans isomer of **1** was isolated. Presumably, the steric demands of the partially twisted 4-PhPy ligand disfavor the formation of the cis complex enough to force the reaction primarily toward trans ligation. Although **1cis** could not be isolated, evidence for its formation as a minority product (ca. 5% relative to **1trans**) was found in the IR spectra of concentrated reaction solutions (not shown). The usefulness of the carbonyl spectrum as a diagnostic is illustrated in Figure 1. Shown in Figure 1 are spectra for **4**, a reaction mixture of **2**, and isolated **2trans** and **2cis** in THF. The trans complex (C_{2h} symmetry) shows three C≡O stretches, while the cis complex (C_{2v}) displays four.

Crystal Structures. Table 1 contains crystal information and refinement data for **1trans**, **2trans**/**2cis**, **3trans**, **3cis**, and **4**. Table 2 lists selected Re—N bond lengths from the five structures. ORTEP drawings for the X-ray crystal structures of **1trans**, **2trans**, **2cis**, **3trans**, **3cis**, and **4** are shown in Figure 2. **4** crystallizes in the $I4_1/a$ space group with no appreciable distortions of the BiBzIm ligand. The Re atoms exist in a slightly distorted octahedral coordination: N—Re—CO bonding angles range between 86.2 and 91.7°, while the N—Re—N angle is 77.82(9)°. The Re—Re distance is 5.72 Å.

1trans crystallizes in the $P2_1/n$ space group with two molecules comprising the asymmetric unit (only one of which is shown in Figure 2). The structure also contains disordered THF and hexane molecules. Notably, there is a slight distortion of the molecule away from an orthogonal ideal such that it adopts a "Z" geometry featuring ligand N—Re—Re angles of about 80°. Evident in the structure are the above-mentioned pyridine/phenyl torsional displacements (ca. 30°) that are likely responsible for the preferential formation of the trans isomer. Re—Re distances are 5.74 and 5.72 Å.

As shown by the packing diagram in Figure 3, **2trans** and **2cis** cocrystallize with the 2,4′-bpy ligands of **2trans**

(21) Abel, E. W.; Wilkinson, G. *J. Chem. Soc.* **1959**, 1501−1505.
(22) Wojcicki, A.; Basolo, F. *J. Am. Chem. Soc.* **1961**, *83*, 525−528.
(23) Angelici, R. J.; Basolo, F. *J. Am. Chem. Soc.* **1962**, *84*, 2495−2499.
(24) Angelici, R. J.; Basolo, F. *Inorg. Chem.* **1963**, *2*, 728−731.
(25) In refluxing toluene, however, only **3trans** is formed when **4** and pyridine are combined.

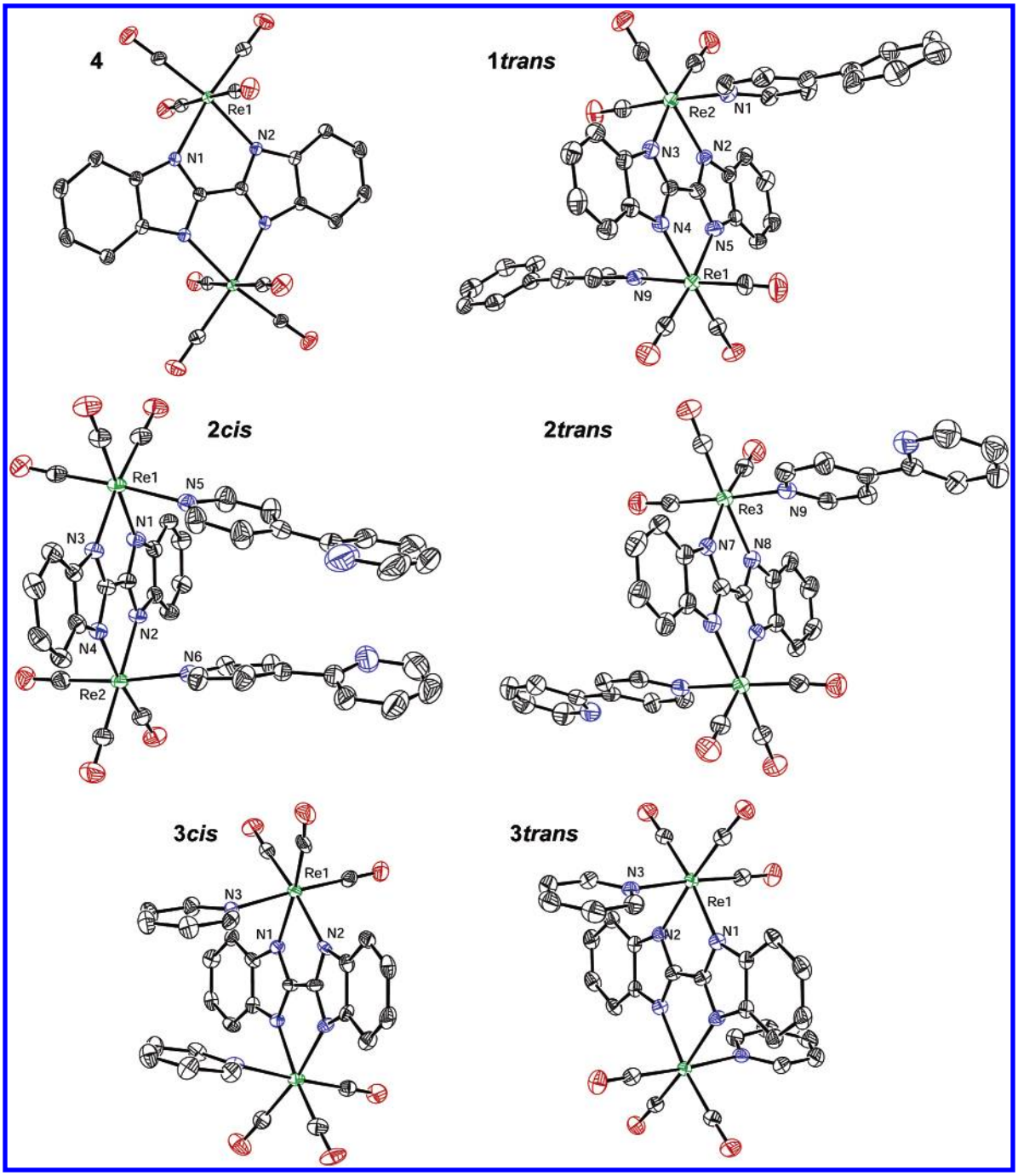

Figure 2. ORTEP renderings of **1trans**, **2trans**, **2cis**, **3trans**, **3cis**, and **4** shown at the 50% probability level. Rhenium atoms are shown in green, nitrogen in blue, oxygen in red, and carbon in black. Hydrogen atoms have been removed for clarity. Only one of the two isomers for **1trans** is shown.

lying across the 2,4′-bpy ligands of **2cis** in a manner that facilitates good van der Waals contact. The compounds crystallize in the $P2_1/n$ space group, where the asymmetric unit contains one half of a molecule of **2trans** and a full molecule of **2cis**. The absence of a proton in one of the meta positions on the second pyridyl ring allows the two rings of 2,4′-bpy to lie nearly planar, likely facilitating cis ligation. The torsion angle between the pyridine rings averages 6° for **2trans** and 11° for **2cis**. Similar to **1trans**, the structure of **2trans** distorts toward a "Z" shape, with 2,4′-bpy N—Re—Re angles of approximately 84°. Slightly larger distortions are seen for **2cis**, where the 2,4′-bpy ligands are bowed toward each other, resulting in 2,4′-bpy N—Re—Re angles of 78.2 and 80.4°. The Re—Re distances in **2trans** and **3cis** are 5.78 and 5.74 Å, respectively.

3trans crystallizes in the $P2_1/n$ space group with distortions similar to those of **1trans** and **2trans** (the pyridine N—Re—Re angle is 83.5°). The Re—Re distance is 5.73 Å. **3cis** crystallizes in the $I\bar{4}2_d$ space group and features slightly larger distortions (inward bowing of pyridine ligands) than those found for **2cis**, where the pyridine ligands bow in toward each other. The pyridine N—Re—Re angle is 75.4°. The Re—Re distance is the shortest of the six molecules at 5.69 Å.

Table 2 contains Re—N bond distances for the six molecules. Both the imidazolyl N—Re and the pyridyl N—Re bond distances [averaging 2.22(1) and 2.21(1) Å,

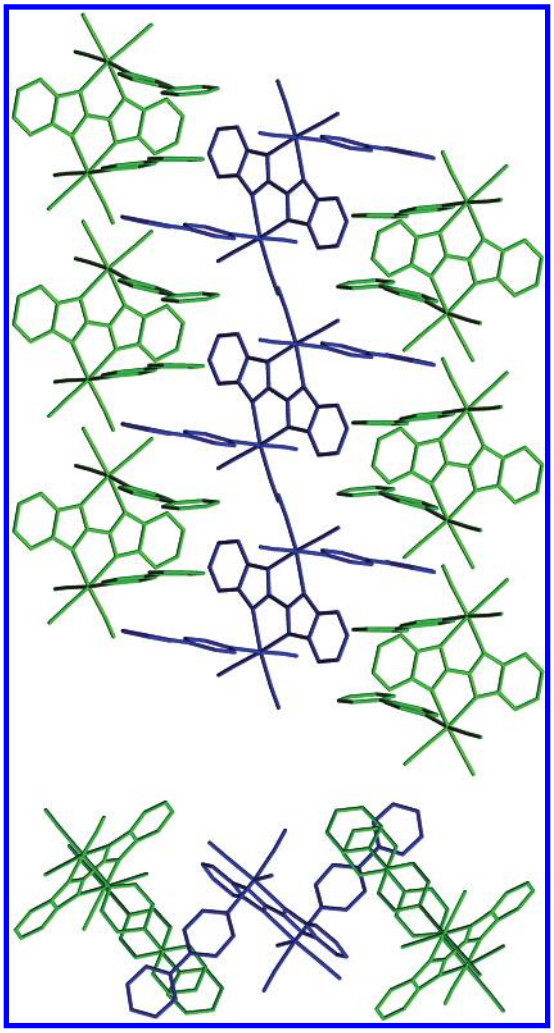

Figure 3. Packing diagram for **2trans**/**2cis** (stick figure renderings). For clarity, **2trans** is shown in blue and **2cis** is shown in green. The top diagram shows a side view and the bottom shows a top view of the packing orientation along the *a* axis. For each molecule of **2trans**, two molecules of **2cis** are interspaced on either side overlapping the 2,4′-bpy ligands and forming columns along the *a* axis.

respectively] are consistent with those found for molecular rectangles synthesized using the $[Re(CO)_3]_2$BiBzIm bridge unit.[1,9]

Electronic Absorption. Figure 4 contains electronic absorption spectra for **4**, **1trans**, **2trans**, **2cis**, **3trans**, and **3cis** in CH_2Cl_2 as the solvent. The spectra are dominated by high energy transitions (<400 nm) associated with the BiBzIm bridging ligand. Notably absent are the distinct visible-region metal-to-ligand charge-transfer (MLCT) transitions ($Re^I \rightarrow L\pi^*$) obtained for analogous molecular rectangles.[1,10] The difunctional ligands of the rectangles are, of course, ligated by two, rather than one, rhenium cations, resulting in lower $L\pi^*$ orbital energies and accounting for the shift of MLCT bands into the visible region.

Electrochemistry. Cyclic voltammograms (CVs) of **1trans**, **2trans**, and **2cis** in THF display chemically reversible reduction waves, while CVs of **4**, **3trans**, and **3cis** show multiple irreversible reduction waves. Figure 5 shows a CV for **4**, **2trans**, and **2cis**. CVs for **1trans**, **3trans**, and **3cis** are included in Supporting Information. Table 3 summarizes

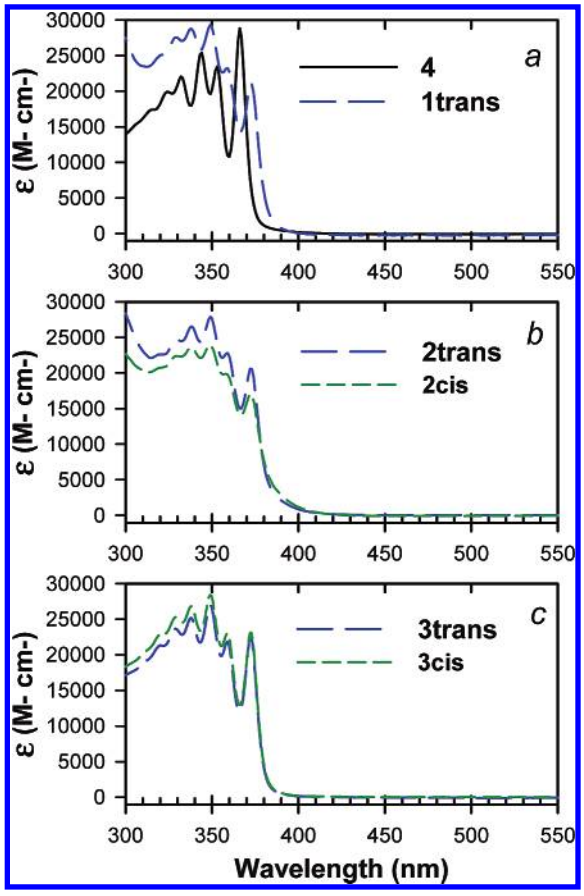

Figure 4. UV−visible absorption spectra obtained in CH_2Cl_2. Panel a shows **4** (solid black line) and **1trans** (long dashed blue line). Panel b shows **2trans** (long dashed blue line) and **2cis** (short dashed green line). Panel c shows **3trans** (long dashed blue line) and **3cis** (short dashed green line).

the reduction potentials for **4**, **1trans**, **2trans**, **2cis**, **3trans**, and **3cis** as well as the reduction potentials for the free ligands.

Visible-region SEC measurements with **2cis** (Figure 6) show the formation of the characteristic absorption spectrum of the 2,4′-bpy radical anion, establishing the 2,4′-bpy ligand as the site of reduction.[26] On the basis of comparative free-ligand reduction potentials, we tentatively ascribe the initial reductions of **1trans**, **3trans**, and **3cis** to pyridyl ligands as well, but we cannot rule out reduction of Re(I) to Re(0), especially where electrochemical irreversibility is encountered. (In these coordination environments, Re(0) represents a 19-electron species and would be expected to display instability and electrochemical irreversibility.)[27] The positive shifts in putative ligand reduction potentials in comparison to free-ligand reductions are understandable on the basis of electrostatic stabilization of the coordinated ligand anion by the cationic metal center. At the same time, the reduction potentials are still considerably more negative than those found for related molecular rectangles, where two metal cations coordinate each ligand. As noted above, the differences in the ease of reduction of the coordinated L in C and

(26) Yang, L.; Wimmer, F. L.; Wimmer, S.; Zhao, J. X.; Braterman, P. S. *J. Organomet. Chem.* **1996**, *525*, 1−8.
(27) Paolucci, F.; Marcaccio, M.; Paradisi, C.; Roffia, S.; Bignozzi, C. A.; Amatore, C. *J. Phys. Chem. B* **1998**, *102*, 4759−4769.

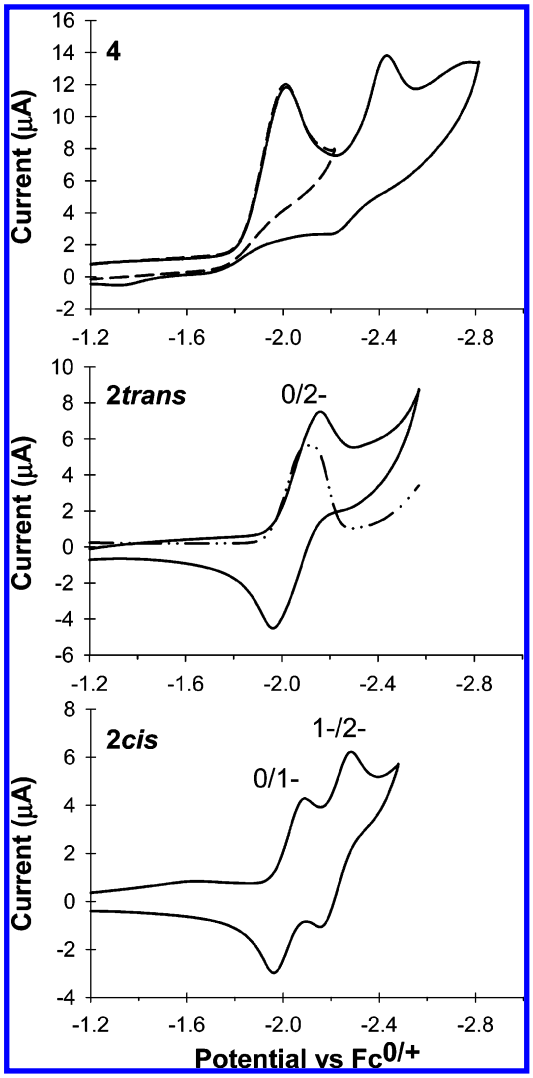

Figure 5. Top graph: CV of **4** at a potential scan rate of 200 mV/s. Middle graph: CV (solid black line) and DPV (dashed−dotted black line) of **2trans**. Bottom graph: CV (solid black line) of **2cis**. All scans were performed in THF with 0.1 M $TBAPF_6$ as the supporting electrolyte and referenced against the ferrocene/ferrocenium couple.

Table 3. Reduction Potentials of **1trans**, **2trans**, **2cis**, **3trans**, **3cis**, and **4** (V vs Fc/Fc^+)[a]

compound	$E_{1/2}^{0/1-}$	$E_{1/2}^{1-/2-}$	ligand	$E_{1/2}^{0/1-}$
1trans	−2.32[b]	−2.42[b]	4-PhPy[d]	−2.62[f]
2trans	−2.07[b]	−2.16[b]	2,4′-bpy[e]	−2.50
2cis	−2.01	−2.18		
3trans	−2.39[c]	−2.54[c]	Py[d]	−3.12[f]
3cis	−2.49[c]			
4	−1.69[c]	−2.07[c]		

[a] In THF with 0.1 M $TBAPF_6$ used as the supporting electrolyte. [b] 0/1− and 1−/2− waves strongly overlap in CV measurements. Values are estimated from Gaussian deconvolutions of the DPV scan. [c] Irreversible reduction wave. Value shown for the peak cathodic wave. [d] Value taken from *J. Chem. Soc. A* **1968**, 381−182. [e] Value taken from ref 26. [f] Converted to $Fc^{0/+}$ reference by subtracting 0.36 from the reported value referenced to Ag/AgCl.

Z versus the ease of reduction of rectangle assemblies are reflected in the absence or presence, respectively, of visible-region MLCT absorption bands.

The more careful inspection of reduction waves for **1trans** and **2trans** indicates that they likely comprise two strongly overlapping single-electron reductions. Differential pulse voltammetry (DPV) scans (see the example in Figure 5) display the broadened peaks and flattened tops expected for closely spaced pairs of reductions. Fits of the scans as overlapping Gaussians yielded formal potential differences, ΔE_f, of 100 and 90 mV, respectively, for the first two reductions of **1trans** and **2trans**, respectively. In contrast, the 0/1− and 1−/2− reductions for **2cis** are separated by 170 mV. For the corresponding 4,4′-bipyridine-based rectangle, they are separated by 230 mV. These translate into LCMV comproportionation constants of 50, 30, 750, and 7700, respectively, for **1trans**, **2trans**, **2cis**, and the 4,4′-bipyridine-based rectangle. The differences are ascribable to variations in the electrostatic interactions between reduced pairs of bipyridyl ligands, the interactions being substantially greater for the proximal pairs found in the cis assembly and the rectangle.

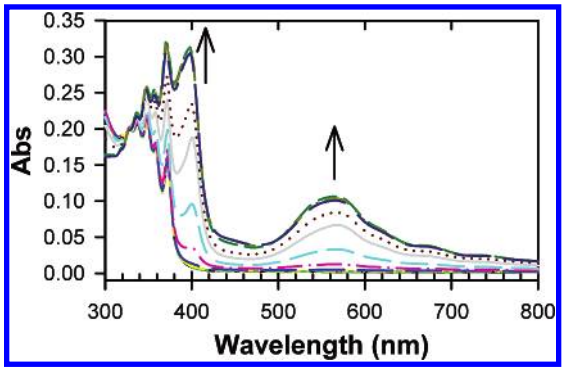

Figure 6. UV/visible SEC measurement of ***2*cis** during the reduction to the 1− state. The new absorption bands at approximately 400 and 560 nm are indicative of the 2,4′-bpy radical anion. The elapsed time for the series of SEC measurements shown was approximately 2 h. Measurements were also made in the extended NIR region (not shown) but did not reveal any new absorption bands.

Finally, returning to spectral measurements, attempts to observe a red or NIR intervalence transition for **2cis** via either SEC or chemical reduction with 5% sodium amalgam were unsuccessful, even at a lower temperature (0 °C). The band presumably exists, but the reduced compound lacks the stability needed over the extended electrolysis times required for the NIR SEC experiments.

Conclusions

Molecules of the form *cis*- and *trans*-$[Re(CO)_3(L)]_2$BiBzIm, where L = 4-PhPy (trans only), 2,4′-bpy, and pyridine, have been synthesized. X-ray crystallography is consistent with the proposed structures. In the case where L = 4-PhPy, the trans isomer is observed in greater than 20:1 excess over the cis isomer, likely reflecting the torsional steric demands of proximal phenylpyridine ligands. The compounds are acyclic analogues of recently studied tetrarhenium molecular rectangles and are of interest because of their potential to form LCMV compounds upon reduction by one electron. SEC measurements corroborated the formation of LCMV versions of *cis*-$[Re(CO)_3(L)]_2$(2,2′-bisbenzimidizolate) but failed to uncover a ligand-based intervalence transition as a result of the instability of the reduced species. Electrochemical measurements revealed isomer-dependent L/L electrostatic effects, resulting in greater mixed-valence ion comproportionation for C- versus Z-shaped assemblies.

Acknowledgment. We thank Baoqing Ma for assistance in the crystallographic refinement of **1trans**. We gratefully acknowledge the Office of Science, U.S. Department of Energy (Grant DE-FG02-87ER13808), for financial support of our research.

Supporting Information Available: X-ray crystallographic files for **1trans**, **2trans/2cis**, **3trans**, **3cis**, and **4** (CIF) and electrochemical data for **1trans**, **3trans**, and **3cis**. This material is available free of charge via the Internet at http://pubs.acs.org.

IC050894U